Physics Letters B 774 (2017) 682–705

Contents lists available at ScienceDirect

Physics Letters B

www.elsevier.com/locate/physletb

Measurement of vector boson scattering and constraints on anomalous quartic couplings from events with four leptons and two jets in proton–proton collisions at $\sqrt{s} = 13$ TeV

The CMS Collaboration ⋆

CERN, Switzerland

ARTICLE INFO

Article history:
Received 9 August 2017
Received in revised form 21 September 2017
Accepted 10 October 2017
Available online 17 October 2017
Editor: M. Doser

Keywords:
CMS
Physics
SM
ZZ
VBS
aQGC

ABSTRACT

A measurement of vector boson scattering and constraints on anomalous quartic gauge couplings from events with two Z bosons and two jets are presented. The analysis is based on a data sample of proton–proton collisions at $\sqrt{s} = 13$ TeV collected with the CMS detector and corresponding to an integrated luminosity of 35.9 fb^{-1}. The search is performed in the fully leptonic final state $\mathrm{ZZ} \to \ell\ell\ell'\ell'$, where $\ell, \ell' = \mathrm{e}$ or μ. The electroweak production of two Z bosons in association with two jets is measured with an observed (expected) significance of 2.7 (1.6) standard deviations. A fiducial cross section for the electroweak production is measured to be $\sigma_{\mathrm{EW}}(\mathrm{pp} \to \mathrm{ZZjj} \to \ell\ell\ell'\ell'\mathrm{jj}) = 0.40^{+0.21}_{-0.16}\,(\mathrm{stat})\ ^{+0.13}_{-0.09}\,(\mathrm{syst})$ fb, which is consistent with the standard model prediction. Limits on anomalous quartic gauge couplings are determined in terms of the effective field theory operators T0, T1, T2, T8, and T9. This is the first measurement of vector boson scattering in the ZZ channel at the LHC.

1. Introduction

Weak vector boson scattering (VBS) plays a central role in the standard model (SM) and is a key process to probe the non-Abelian gauge structure of the electroweak (EW) interaction. In the absence of any other contributions, the scattering amplitude of longitudinally polarized vector bosons would violate unitarity at center-of-mass energies for the scattering process of order 1 TeV [1,2]. The discovery of a scalar boson at the CERN LHC [3,4] with gauge couplings compatible with those predicted for the SM Higgs boson [5] provides evidence that contributions from the exchange of this boson may be responsible for preserving unitarity at high energies, as predicted in the SM.

Unitarity restoration for longitudinal boson scattering in the SM relies on the interference of the VBS amplitudes and amplitudes that involve the Higgs boson. Any deviation in the SM coupling of the Higgs boson to the gauge bosons breaks this delicate cancellation, thus permitting a test of the EW symmetry breaking mechanism (EWSB) of the SM. The study of differential cross sections for VBS processes at large diboson invariant masses provides a model-independent test of the Higgs boson couplings to vector bosons, complementing direct measurements of Higgs boson production and decay rates. Many models of physics beyond the SM alter the couplings of vector bosons, and the effects can be parametrized in an effective field theory approach [6]. The VBS topology increases the sensitivity to the contribution of the quartic interactions, allowing tests for the presence of anomalous quartic gauge couplings (aQGCs) [7].

At the LHC, VBS is initiated by quarks q from the colliding protons; both quarks radiate vector bosons (V = W, Z) which then interact. Because of the relatively small transverse momentum p_{T} carried by the gauge bosons and the absence of any color exchange at leading order (LO), VBS is characterized by the presence of two forward jets j in addition to the outgoing gauge bosons ($\mathrm{qq} \to \mathrm{VVjj}$) and little hadronic activity between the two jets [8,9]. The hard interaction in VBS only involves the EW interaction. Fig. 1 shows some of the Feynman diagrams that contribute to the EW production of the VVjj signature, involving quartic (top left) and trilinear vertices (top right), as well as diagrams involving the Higgs boson (bottom left). The $\mathrm{qq} \to \mathrm{VVjj}$ process can also be mediated through the strong interaction (bottom right in Fig. 1), which leads to the same final state as the VBS signal, resulting in an irreducible background.

Both the ATLAS and CMS Collaborations performed searches for VBS using proton–proton collisions at $\sqrt{s} = 8$ TeV, notably in the same-sign WW channel [10–12]. The ATLAS Collaboration also re-

⋆ *E-mail address:* cms-publication-committee-chair@cern.ch.

https://doi.org/10.1016/j.physletb.2017.10.020

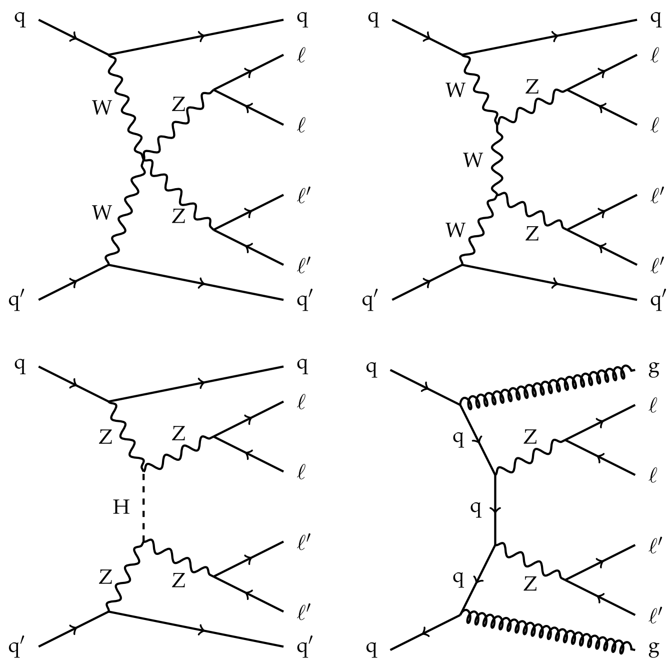

Fig. 1. Representative Feynman diagrams for the EW- (top row and bottom left) and QCD-induced production (bottom right) of the $ZZjj \to \ell\ell\ell'\ell'jj$ (ℓ, $\ell' = e$ or μ) final state. The scattering of massive gauge bosons as depicted in the top row is unitarized by the interference with amplitudes that feature the Higgs boson (bottom left).

ported limits on a fiducial cross section for VBS in the WZ channel [13]. The ZZ channel remained unprobed. Limits on aQGCs are reported in Refs. [10–18].

This paper presents the first experimental investigation of VBS in the ZZ channel and exploits the fully leptonic final state, where both Z bosons decay into electrons or muons, $ZZ \to \ell\ell\ell'\ell'$ (ℓ, $\ell' =$ e or μ). Despite a low cross section, a small $Z \to \ell\ell$ branching fraction, and a large irreducible QCD background, this channel provides a favorable laboratory to study EWSB because all final-state particles are reconstructed. The clean leptonic final state results in a small reducible background, where one or more of the reconstructed lepton candidates originate from the misidentification of jet fragments. This channel also provides a precise knowledge of the scattering energy. Furthermore, the spin correlations of the reconstructed fermions permit the extraction of the longitudinal contribution to VBS.

The search for the EW production of the $\ell\ell\ell'\ell'$jj final state is carried out using pp collisions at $\sqrt{s} = 13$ TeV recorded with the CMS detector at the LHC. The data set corresponds to an integrated luminosity of 35.9 fb^{-1} collected in 2016. A multivariate discriminant, which combines observables sensitive to the kinematics of the VBS process to separate the EW- from the QCD-induced production, is used to extract the signal significance and to measure the cross section for the EW production in a fiducial volume. Finally, the selected $\ell\ell\ell'\ell'$jj events are used to constrain aQGCs described by the operators T0, T1, and T2 as well as the neutral-current operators T8 and T9 [7].

2. The CMS detector

The central feature of the CMS apparatus is a superconducting solenoid of 6 m internal diameter, providing a magnetic field of 3.8 T. Within the solenoid volume are silicon pixel and strip tracking detectors, a lead tungstate crystal electromagnetic calorimeter (ECAL), and a brass and scintillator hadron calorimeter (HCAL), each composed of a barrel and two endcap sections. Forward calorimeters extend the pseudorapidity η coverage provided by the barrel and endcap detectors up to $|\eta| < 5$. Muons are measured in gas-ionization detectors embedded in the steel flux-return yoke outside the solenoid.

The silicon tracker measures charged particles within the pseudorapidity range $|\eta| < 2.5$. It consists of 1440 silicon pixel and 15 148 silicon strip detector modules. For nonisolated particles with $1 < p_T < 10$ GeV and $|\eta| < 1.4$, the track resolutions are typically 1.5% in p_T and 25–90 (45–150) μm in the transverse (longitudinal) impact parameter [19].

Electrons are measured in the pseudorapidity range $|\eta| < 2.5$ using both the tracking system and the ECAL. The momentum resolution for electrons with $p_T \approx 45$ GeV from $Z \to e^+e^-$ decays ranges from 1.7% for nonshowering electrons in the barrel region ($|\eta| < 1.479$) to 4.5% for showering electrons in the endcaps [20].

Muons are measured in the pseudorapidity range $|\eta| < 2.4$ using the silicon tracker and muon systems. The muon detectors are constructed using three different technologies: drift tubes for $|\eta| < 1.2$, cathode strip chambers for $0.9 < |\eta| < 2.4$, and resistive plate chambers for $|\eta| < 1.6$. In the intermediate p_T range of $20 < p_T < 100$ GeV, matching muons to tracks measured in the silicon tracker results in a relative p_T resolution of 1.3–2.0% in the barrel ($|\eta| < 1.2$), and better than 6% in the endcaps. The p_T resolution in the barrel is better than 10% for muons with p_T up to 1 TeV [21].

In the region $|\eta| < 1.74$, the HCAL cells have widths of 0.087 in pseudorapidity and 0.087 in azimuth (ϕ). In the η–ϕ plane, and for $|\eta| < 1.48$, the HCAL cells map on to 5×5 arrays of ECAL crystals to form calorimeter towers projecting radially outwards from the nominal interaction point. For $|\eta| > 1.74$, the size of the towers increases progressively to a maximum of 0.174 in $\Delta\eta$ and $\Delta\phi$. When combining information from the entire detector, the jet energy resolution amounts typically to 15% at 10 GeV, 8% at 100 GeV, and 4% at 1 TeV, to be compared to about 40%, 12%, and 5% obtained when the ECAL and HCAL calorimeters alone are used.

The first level of the CMS trigger system, composed of custom hardware processors, uses information from the calorimeters and muon detectors to select events of interest in a fixed time interval of 3.2 μs. The high-level trigger processor farm further decreases the event rate from around 100 kHz to less than 1 kHz, before data storage [22].

A more detailed description of the CMS detector, together with a definition of the coordinate system used and the relevant kinematic variables, can be found in Ref. [23].

3. Signal and background simulation

Several Monte Carlo event generators are used to simulate the signal and background contributions. The simulated samples are employed to optimize the event selection, to develop the multivariate discriminator, and to estimate the irreducible background yields.

The EW production of Z boson pairs and two final-state quarks, where the Z bosons decay leptonically, is simulated at LO using MadGraph5_amc@nlo v2.3.3 (abbreviated as MG5_aMC in the following) [24]. The sample includes triboson processes, where the Z boson pair is accompanied by a third vector boson that decays into jets, as well as diagrams involving the quartic coupling vertex. The predictions from this sample are cross-checked with those obtained from the LO generator Phantom v1.2.8 [25], and excellent agreement in the yields and the multivariate distribution exploited for the signal extraction is found.

The event samples of the QCD-induced production of two Z bosons are simulated with zero, one, and two outgoing partons